A microscopic Monte Carlo approach to modeling of Resistive Plate Chambers

A microscopic Monte Carlo approach to modeling of Resistive Plate Chambers

2014 JINST 9 P09012

(http://iopscience.iop.org/1748-0221/9/09/P09012)

PUBLISHED BY IOP PUBLISHING FOR SISSA MEDIALAB

RECEIVED: *May 26, 2014*
ACCEPTED: *August 13, 2014*
PUBLISHED: *September 22, 2014*

A microscopic Monte Carlo approach to modeling of Resistive Plate Chambers

D. Bošnjaković,[a,b,1] **Z.Lj. Petrović**[a,b] **and S. Dujko**[a]

[a] *Institute of Physics,*
University of Belgrade, Pregrevica 118, 11070 Belgrade, Serbia
[b] *Faculty of Electrical Engineering,*
University of Belgrade, Bulevar kralja Aleksandra 73, 11120 Belgrade, Serbia

E-mail: dbosnjak@ipb.ac.rs

ABSTRACT: We present a "microscopic" approach in modeling of Resistive Plate Chambers where individual electrons and their collisions with the gas molecules are followed using a Monte Carlo simulation technique. Timing resolutions and efficiencies are calculated for a specific timing RPC with 0.3 mm gas gap and gas mixture of 85% $C_2H_2F_4$ + 5% iso-C_4H_{10} + 10% SF_6. Calculations are performed for different sets of cross sections for electron scattering in $C_2H_2F_4$ and primary cluster size distributions. Results of calculations are compared with those obtained in experimental measurements. Electron avalanche fluctuations are also studied and compared with analytical models.

KEYWORDS: Resistive-plate chambers; Detector modelling and simulations II (electric fields, charge transport, multiplication and induction, pulse formation, electron emission, etc); Charge transport and multiplication in gas; Gaseous detectors

[1] Corresponding author.

doi:10.1088/1748-0221/9/09/P09012

2014 JINST 9 P09012

Contents

1 Introduction

Developed in the 1980s [1, 2], Resistive Plate Chambers (RPCs) became widely used particle detectors in high energy physics experiments [3–5]. Electrodes of highly resistive material, such as glass or bakelite, make them free from destructive discharges. They also show remarkable timing resolutions of about 50 ps [6]. Due to their simple construction and low cost, they are often used for large area timing and triggering purposes, but other applications such as medical imaging were also considered [7].

Despite their apparent simplicity, modeling of RPCs is not an easy task because of various physical phenomena ranging from charge generation, transport and multiplication, to signal induction, propagation and electrode relaxation effects, all occurring on different time scales. Yet, many RPC models were developed and published [8]. Most numerical models are based on either the Monte Carlo simulation technique [9, 10] or on the fluid equations [11, 12]. The latter can only provide the mean values of RPC signals in a deterministic fashion while the Monte Carlo models usually follow some theoretical distributions for primary ionization and electron avalanche fluctuations in order to calculate the RPC performance characteristics such as timing resolution, efficiency and charge spectrum. On the other hand, while often being approximate, only the analytical models [13, 14] can provide general conclusions about the influence of different parameters on the RPC performance. These models can also include the stochastic effects in physics of RPCs.

Every RPC model relies on accurate data for electron swarm transport in gases. These parameters include the transport coefficients (e.g. drift velocity and diffusion coefficients) and rate coefficients (e.g. attachment and ionization rate) which are usually calculated from electron impact cross sections using a computer code based on either Monte Carlo method or Boltzmann equation

2014 JINST 9 P09012

analysis. A Monte Carlo code that is often used for such purpose — MAGBOLTZ 2 [15, 16] has cross sections imbedded into the code. Thus cross sections cannot be easily modified, compared or presented. The questions associated with the reliability of cross sections for electron scattering in RPC's gases were already raised in case of $C_2H_2F_4$ [17], which is the main component in gas mixtures for RPCs operated in avalanche mode. As will be shown, the final results that describe the RPC performance may differ considerably depending on the cross sections used.

In this paper, we follow a completely different approach in RPC modeling. Our approach is based on 3D tracking of individual electrons and their collisions with the background gas in a typical Monte Carlo fashion. Here the avalanche fluctuations and the RPC performance characteristics emerge naturally from the stochastic character of electron collisions and are determined exclusively by the cross sections for electron scattering. Such an approach based on MAGBOLTZ was used for the calculation of gas gain fluctuations [18] but still, no such attempts in RPC modeling were published [17].

This paper is organized as follows. First, we discuss our simulation technique (section 2). Then, we present the results for electron avalanches in an infinite space (sections 3.2 and 3.3) which are used for comparison with the analytical models of avalanche development and timing. Finally, the boundaries are introduced (section 3.4) and timing and efficiency are calculated for a specific timing RPC (0.3 mm gas gap, gas mixture of 85% $C_2H_2F_4$ + 5% iso-C_4H_{10} + 10% SF_6). A study is made with different cross section sets and cluster size distributions. The results are compared with experimental values. Due to limited computing resources we are only able to use a relatively low value of signal threshold of about 10^6 electrons which excludes the space charge effects.

2 Simulation technique

Our simulation technique for an RPC event (i.e. passage of an incoming particle) can be divided into a few steps. First, we generate the primary ionization, e.g., the initial electrons due to passage of the incoming particle. The individual electrons and their collisions with the background gas are then traced between the moments of sampling. In these moments, we record some quantities (e.g. number of electrons) and calculate the induced signal. Sampling interval is set to 0.2 ps. The threshold crossing time is determined using the exponential interpolation between the samples. The simulation consisting of 10000 events usually takes approximately two days of computation time on a multiprocessor system with about 300 active CPU cores @ 2.1 GHz.

2.1 Primary ionization

Primary ionization is generated according to a commonly used model. The primary electrons are grouped in clusters. Electrons belonging to the same cluster have the same initial position. Number of electrons in the cluster is generated using a cluster size distribution. The positions of the clusters are generated using exponential distribution for the distance between neighboring clusters

$$P(x) = \frac{1}{\lambda} \exp\left(-\frac{x}{\lambda}\right),$$

where λ is the mean distance between clusters. Initial velocity of primary electrons is chosen according to the Maxwellian velocity distribution with the mean electron energy of 1 eV. Mean

2014 JINST 9 P09012

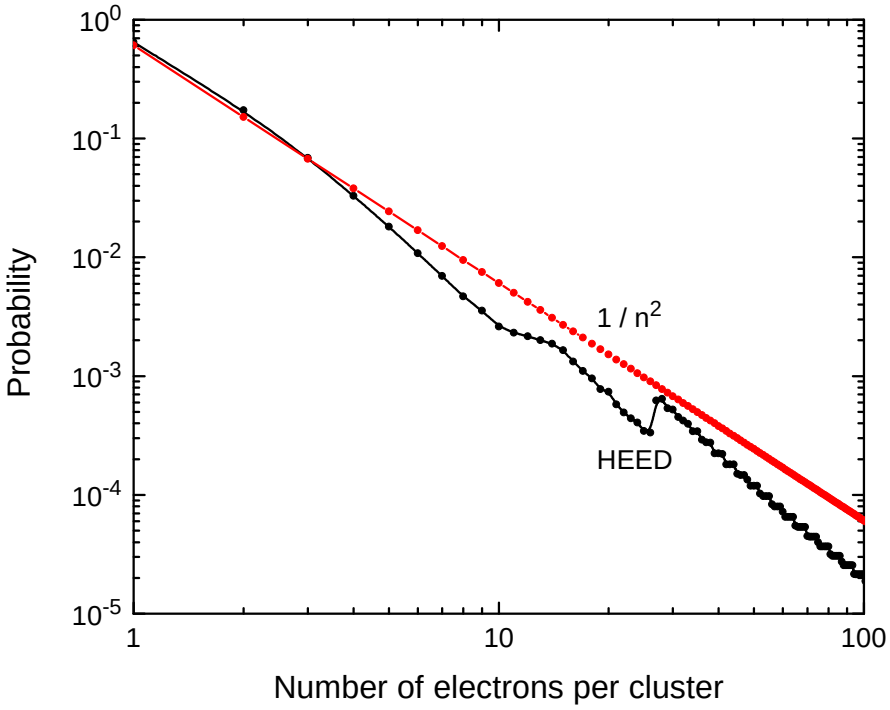

Figure 1. Cluster size distribution calculated by HEED, and $1/n^2$ model.

distance between the clusters and cluster size distribution are calculated using a computer program HEED [19, 20]. For minimum ionizing particles, we have obtained a value of 8.44 clusters/mm, which differs from 7.5 clusters/mm quoted in [21]. Considering the arguments and measurements presented in [21], we have decided to use the value of 7.5 clusters/mm since it seems more realistic. For cluster size distributions we use two models in our simulations for comparison: the $1/n^2$ model and the distribution calculated by HEED (figure 1). Both distributions are cut to 500 electrons.

2.2 Electron tracking

In the work reported here, the Monte Carlo method is used to simulate the motion of electrons in the background gas. In the present Monte Carlo code both elastic and inelastic collisions are assumed to occur in the interactions of the electrons with the gas molecules. The electron-electron interactions are neglected since the transport is considered in the limit of low electron density. Calculations are performed at zero gas temperature and isotropic scattering is assumed to occur in all electron-molecule collisions regardless of the nature of specific processes or energy.

Spatiotemporal evolution of each electron is followed through a time step determined from the mean free time between collisions. This small time step is used to solve the integral equation for the collision probability in order to determine the time of the next collision. This can be done using either the null collision technique or integration technique. In our code (and in contrast to MAGBOLTZ) the latter approach is employed. The number of time steps is determined in such a way as to optimize the performance of the Monte Carlo code without reducing the accuracy of the final results. After a collision has occurred, it is then determined whether the electron has collided elastically or experienced one of the several possible types of inelastic events, by using the relative

2014 JINST 9 P09012

probabilities of various collision types. When an elastic collision has occurred, the electron energy is reduced by the amount $2m/M$ where m and M are the electron and molecule masses, respectively. In an inelastic collision the electron is assumed to lose an amount of energy corresponding to the energy loss for that particular process. After ionization, it is assumed that all fractions of the distribution of the available energy are equally probable between primary and secondary electrons. When electron attachment takes place, the consumed electron is simply removed from the simulation. Under the hypothesis of isotropic scattering, the change in direction of the electron velocity after a collision is expressed by uniformly distributed scattering angle within interval $[0,\pi]$ and by the azimuthal angle uniformly distributed within the interval $[0,2\pi]$. For more details on our Monte Carlo simulation technique the reader is referred to our recent reviews [22–24].

In the present work we have employed three different sets of cross sections for electron scattering in $C_2H_2F_4$: 1) a set recently developed by our group [25], 2) a set from MAGBOLTZ 2.8.9 (2010), and 3) a set from MAGBOLTZ 2.7.1 (pre-2010). The set developed by our group and the set from MAGBOLTZ 2.8.9 have been recently updated and modified on the basis of new experimental measurements of electron transport data in $C_2H_2F_4$ under the pulsed Townsend conditions [26]. For electron scattering in iso-C_4H_{10}, we have used a set of cross sections from MAGBOLTZ 2.7.1. There is an updated version of the same cross sections hard-coded in more recent versions of MAGBOLTZ but our calculations have revealed much better agreement between our data for ionization coefficient and those experimentally measured [27], if the cross sections from MAGBOLTZ 2.7.1 are considered [27, 28]. Finally, for electron scattering in SF_6 we have employed a set of cross sections developed by Itoh et al. [29].

2.3 Signal induction

The induced current in an electrode is calculated using Ramo's theorem [30]:

$$i(t) = \frac{E_w}{V_w} \cdot q \cdot n(t) \cdot w(t)\,,$$

where E_w is the weighting field of the electrode (calculated as electric field in the gas gap when the electrode is raised to the potential of V_w while the other electrodes are grounded), q is the electron charge, and n is the number of electrons and w represents the flux drift velocity. The flux drift velocity is the average electron velocity while the bulk drift velocity is defined as velocity of center of mass of the electron swarm (avalanche) [31, 32]. The two may differ quantitatively and sometimes even qualitatively when non-conservative collisions such as attachment and/or ionization are present [33]. For our RPC geometry (0.3 mm gas gap, one metallic and one 3 mm thick glass electrode with $\epsilon_r = 8$) the weighting field of 1.48/mm was calculated. The induced charge is calculated as an integral of the induced current, $q(t) = \int_0^t i(\tau)\,d\tau$.

3 Results and discussion

3.1 Preliminaries

First we give a brief summary of the most important parameters used in the following sections. We consider the gas mixture of 85% $C_2H_2F_4$, 5% iso-C_4H_{10} and 10% SF_6 and the gas number density is set to $N = 2.505 \cdot 10^{25}$ m^{-3} which corresponds to the pressure of 1 atm and temperature of 20 °C).

2014 JINST 9 P09012

Table 1. Calculated $S = (\alpha - \eta)w$ and $k = \eta/\alpha$ parameters for a mixture of 85% $C_2H_2F_4$ + 5% iso-C_4H_{10} + 10% SF_6 with three different $C_2H_2F_4$ cross section sets. All calculations presented here are made using our Monte Carlo method.

E/N	*Our set*		*MAGBOLTZ 2.8.9 set*		*MAGBOLTZ 2.7.1 set*	
(Td)	S (10^{10} s^{-1})	k	S (10^{10} s^{-1})	k	S (10^{10} s^{-1})	*k*
359	1.27 ± 0.04	0.20 ± 0.01	1.40 ± 0.04	0.16 ± 0.01	1.66 ± 0.04	0.16 ± 0.01
385	1.62 ± 0.04	0.16 ± 0.01	1.77 ± 0.04	0.13 ± 0.01	2.14 ± 0.04	0.13 ± 0.01
412	2.01 ± 0.04	0.13 ± 0.01	2.20 ± 0.04	0.10 ± 0.01	2.68 ± 0.05	0.10 ± 0.01
439	2.43 ± 0.05	0.11 ± 0.01	2.67 ± 0.05	0.08 ± 0.01	3.26 ± 0.05	0.08 ± 0.01

The reduced electric field E/N is expressed in Td (1 Td = 10^{-21} Vm^2). The primary ionization is generated assuming the mean value of 7.5 clusters/mm for minimum ionizing particles. Velocity of the initial electron(s) is chosen according to the Maxwellian velocity distribution with the mean starting energy of 1 eV. Induced signal is calculated using the weighting field of $E_w/V_w = 1.48/\text{mm}$. The gas gap is 0.3 mm.

Our simulation results are compared with those obtained in an analytical model for time response functions [13]. The model shows that, except for small thresholds (e.g. less than 1000 electrons), the RPC time response function can be written as

$$\rho(n_{\text{th}},t) = \frac{1}{2\pi i}\oint_{|z|=r} \frac{\exp(n_{\text{cl}}F(z))-1}{\exp(n_{\text{cl}})-\exp(n_{\text{cl}}F(1/k))}\frac{(1-k^2)n_{\text{th}}S}{(1-kz)^2}\cdot \\ \cdot\exp\left(-St - n_{\text{th}}\frac{(1-k)(1-z)}{1-kz}\exp(-St)\right)dz, \tag{3.1}$$

where n_{th} and n_{cl} are the threshold given as number of electrons and the mean number of clusters (in our simulation $2.25 = 7.5/\text{mm} \cdot 0.3$ mm gas gap), respectively; $F(z)$ and $S = (\alpha - \eta)w$ are the Z-transform of cluster size distribution with radius of convergence r_F and the effective ionization rate, respectively; α and η are the ionization coefficient and attachment coefficient, respectively; and w is the flux drift velocity and $k = \eta/\alpha$. The integration is made over a circle with radius $r_F < r < 1/k$. Using the expression (3.1), it can easily be shown that the shape of the time response function does not depend on the threshold level. It is only shifted in time, and thus the timing resolution does not depend on the threshold. This is a well know experimental observation [6]. One should note that this model does not include the space charge effects and the effects induced by the gas gap boundaries, i.e. an infinite space is assumed. In addition, when comparison is made with our timing distributions, the theoretical time response functions (3.1) are shifted in time so that their mean threshold crossing time is equal to that of simulated data. Table 1 shows the S and k parameters for different $C_2H_2F_4$ cross section sets and electric field strengths calculated using our Monte Carlo method described in section 2.2.

The analytical model presented above is based on the Legler's basic theory of avalanche statistics [34]. This theory is also used by some other analytical and numerical models [8]. According to this theory the probability for an avalanche, initiated by one electron, to have n electrons after

2014 JINST 9 P09012

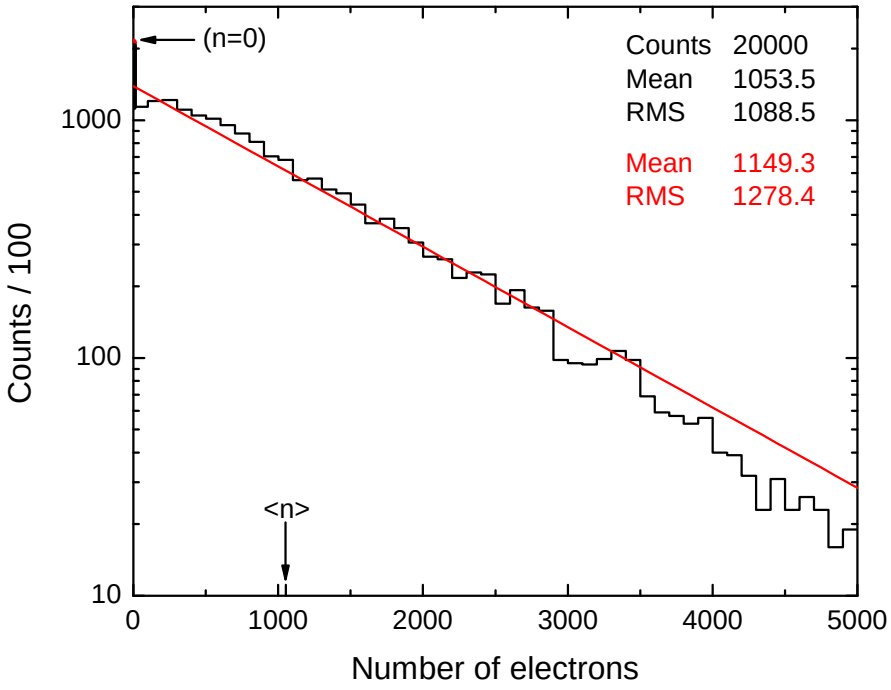

Figure 2. Avalanche size distribution at $t = 290$ ps. (Red) comparison with Legler's model (3.2). Our cross sections for $C_2H_2F_4$ [25] are assumed. $E/N = 439$ Td.

path x is given by

$$P(n,x) = \begin{cases} k\,\dfrac{\bar{n}(x)-1}{\bar{n}(x)-k}, & n=0 \\ \bar{n}(x)\left(\dfrac{1-k}{\bar{n}(x)-k}\right)^2\left(\dfrac{\bar{n}(x)-1}{\bar{n}(x)-k}\right)^{n-1}, & n>0 \end{cases} \tag{3.2}$$

where $\bar{n}(x) = \exp((\alpha-\eta)x)$ is the mean avalanche size at the position x. This distribution has a characteristic exponential shape which has been experimentally confirmed for many gases at lower electric field strengths. But at higher electric fields, a prominent deviation was noticed and could be attributed to the approximation of constant ionization coefficient used by this model [35]. Also, one should bear in mind that x is the position of avalanche center of mass and therefore α and η should be regarded as "bulk" coefficients, i.e. calculated using the bulk drift velocity. However, if the probability $P(n,x)$ is considered as time dependent (3.1), then the distinction between flux and bulk values is not necessary since in each case $\bar{n}$ reduces to $\bar{n}(t) = \exp(St)$ where S is the effective ionization rate.

3.2 Single-electron avalanches

First we present the results of simulation for 20000 avalanches in an infinite space initiated by a single electron. The results for the avalanche size distribution (figure 2) are useful for comparison with Legler's theory of avalanche statistics which is often used in many RPC simulations and modeling [8]. Results show a deviation from the predicted exponential dependence (3.2) mostly prominent at small avalanche sizes. This deviation follows from an approximation of constant first

2014 JINST 9 P09012

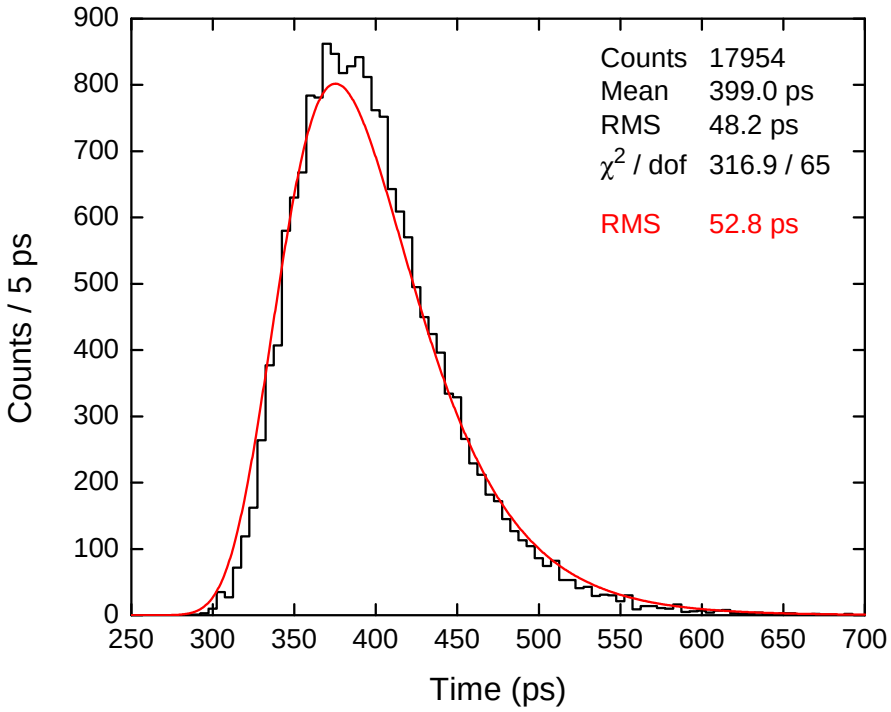

Figure 3. Timing distribution for single electron avalanches. The threshold is set to 10000 electrons and our cross sections for $C_2H_2F_4$ [25] are assumed. $E/N = 439$ Td.

Townsend ionization coefficient, assumed by Legler's basic model. In reality, however, the ionization coefficient varies during avalanche development, especially in the initial stages where only one or just a few electrons are present. Without going into further details, it should be mentioned that there have been several attempts to describe and to deal with this issue in Legler's theory [36]. Unfortunately, even after setting aside the question of their validity and justification, each of these attempts makes the solution for the avalanche size distribution unobtainable in closed form. On the other hand, microscopic Monte Carlo approach does not have to deal with these approximations since the avalanche statistics arise naturally from the stochastic character of electron-molecule collisions. This is the key difference between our model and the other RPC models based on theoretical avalanche size distributions (mostly Legler or Polya type).

Figure 3 shows the timing distribution for a threshold of 10000 electrons. The expected theoretical distribution was calculated using the time response function for the case of single electron avalanches [13]:

$$\rho(n_{\mathrm{th}},t) = \frac{n_{\mathrm{th}} S(1-k)}{1-\exp(-n_{\mathrm{th}}(1-k))} \exp\left(-St - n_{\mathrm{th}}(1-k)\exp(-St)\right) .$$

The slight disagreement with the theoretical distribution can be attributed to the same cause as the disagreement between avalanche size distributions discussed in the previous paragraph. Since the corresponding theoretical avalanche size distribution is "wider" (i.e. has larger standard deviation) than the simulated one, we expected the same for the timing distribution, which is the case. A test was also made with different energy distribution for the initial electron as in the late stage of avalanche development (mean energy of 6.7 eV). The test showed that the higher initial electron en-

2014 JINST 9 P09012

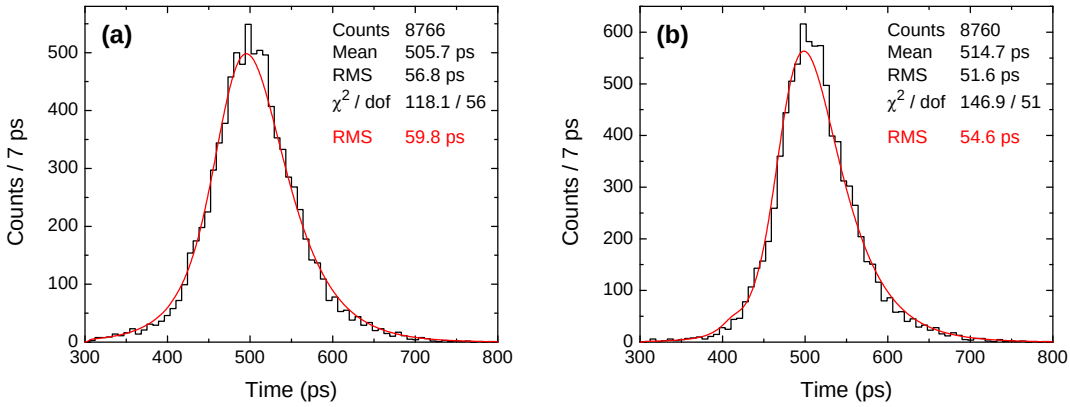

Figure 4. Timing distribution for avalanches started by primary ionization generated using (a) $1/n^2$, (b) HEED cluster size distribution. Infinite space. The threshold is set to 10^6 electrons and our cross sections for $C_2H_2F_4$ [25] are assumed. $E/N = 439$ Td.

ergy had practically no effect on the r.m.s. value of threshold crossing times (it was lower by 0.2 ps) while the number of avalanches which reached the threshold was slightly higher (18350). The latter was expected since the initial electron with higher energy had a lower probability for attachment.

3.3 Avalanches started by primary ionization

The case of avalanches started by primary ionization progressing in an infinite space was also studied. The primary ionization was generated according to the model described in section 2.1. Simulations with 10000 events were made for $1/n^2$ and HEED cluster size distributions. Figure 4 shows the timing distribution for a threshold of 10^6 electrons. The theoretical distributions were calculated using the model (3.1). Slightly higher theoretical r.m.s. values have already been discussed in the previous section. As of distribution shape, one can see that the left tail of the distribution for the $1/n^2$ case is wider than in the case where HEED cluster size distribution was used. This is expected since the left tail represents the fastest events which most often come from high primary ionization, and the probability for large primary clusters is higher in the case of $1/n^2$ distribution (figure 1). The same reasoning applies for the difference between r.m.s. values for the $1/n^2$ and HEED case.

3.4 Full model with primary ionization and boundaries

We now consider the effects of boundaries with gas gap set to 0.3 mm. Avalanches initiated by primary ionization move towards the anode due to electric field. When an electron reaches the anode it is removed from the simulation. Figure 5 shows the results for timing distribution with a threshold of 10^6 electrons. Since the simulation also consists of 10000 events, comparing the number of events which reached the threshold with the one from the previous case without boundaries, one can see the "absorbing effect" of the anode. Also, a slightly higher r.m.s. value can be attributed to the uncertainty of cluster positions, especially the ones closest to the anode which are the first to be absorbed.

The same simulation was performed for a threshold of 2 fC of induced charge. This value corresponds to about 10^6 electrons in the gas gap when the threshold is reached. One could expect

2014 JINST 9 P09012

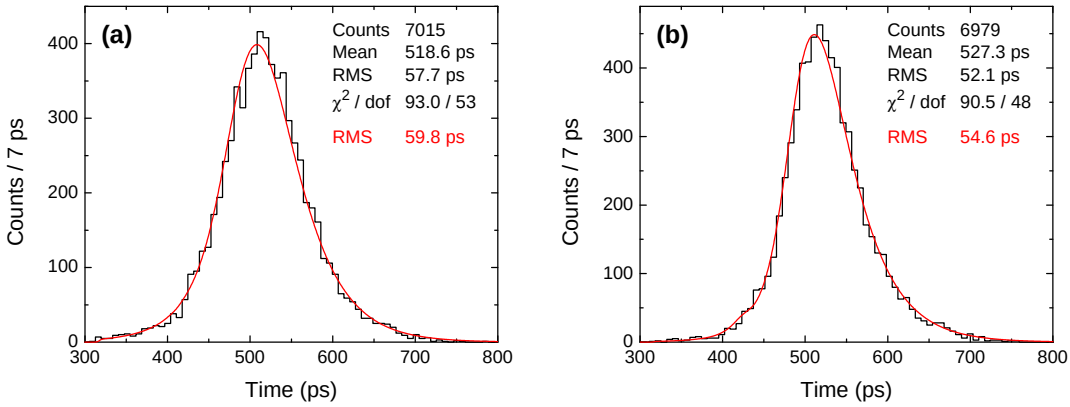

Figure 5. Timing distribution for avalanches started by primary ionization generated using (a) $1/n^2$, (b) HEED cluster size distribution. Gas gap 0.3 mm. The threshold is set to 10^6 electrons and our cross sections for $C_2H_2F_4$ [25] are assumed. $E/N = 439$ Td.

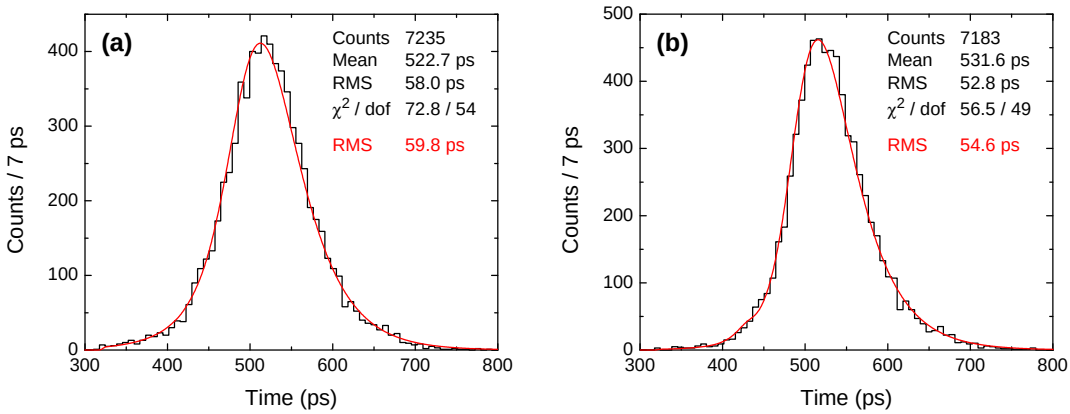

Figure 6. Timing distribution for avalanches started by primary ionization generated using (a) $1/n^2$, (b) HEED cluster size distribution. Gas gap 0.3 mm. The threshold is set to 2 fC and our cross sections for $C_2H_2F_4$ [25] are assumed. $E/N = 439$ Td.

somewhat different results when boundaries are present, because this time the threshold is given by induced charge i.e. the integral of the induced current (which is proportional to the number of electrons in the gas gap). However, the results for this case (figure 6) show that practically only the number of events which reached the threshold is slightly higher than in the case when the threshold is 10^6 electrons. A possible explanation lies in the cumulative character of the induced charge in such way that the avalanches which are absorbed in the anode are not completely "lost" as if they were not present at all. Instead, they contribute to the induced charge, and the other avalanches which would otherwise be too small or too close to the anode to reach the threshold alone, can also contribute so that eventually the threshold is reached.

Finally, we present the results for timing resolution (figure 7) and efficiency (figure 8) of the RPC. The results were made for a range of electric field strengths, different $C_2H_2F_4$ cross section sets and primary cluster size distributions. For each set of parameters 10000 events were simulated with the threshold set to 2 fC. The timing resolution is simply the r.m.s. of the threshold crossing times while the efficiency is the fraction of events which have reached the threshold. Results are

2014 JINST 9 P09012

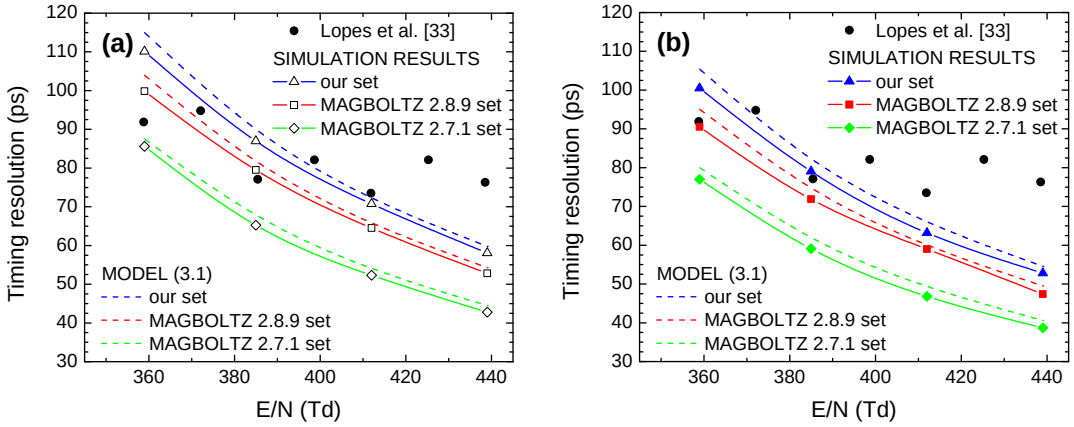

Figure 7. Timing resolutions for different $C_2H_2F_4$ cross section sets and primary ionization models, (a) $1/n^2$, (b) HEED cluster size distribution. Comparison with experimental values by Lopes et al. [37].

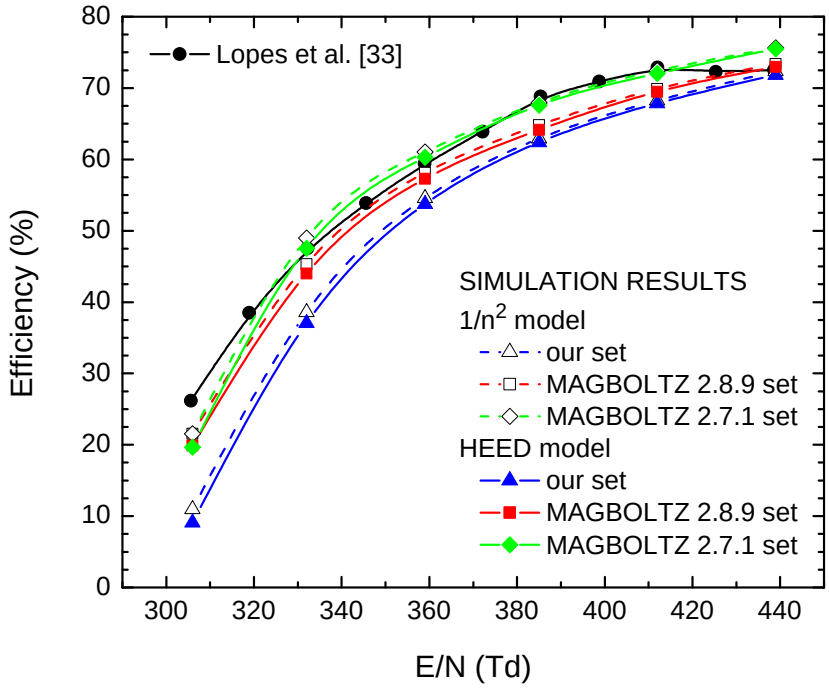

Figure 8. Efficiencies for different $C_2H_2F_4$ cross section sets and primary ionization models, (a) $1/n^2$, (b) HEED cluster size distribution. Comparison with experimental values by Lopes et al. [37].

compared with measurements by Lopes et al. [37] which show a clear fluctuation of the timing resolution, probably due to some kind of experimental uncertainty. Also, the measured timing resolutions and efficiencies both show a pronounced saturation effect at higher electric field strengths which is not present in our results. The theoretical timing resolutions, calculated using (3.1), are in good agreement with the simulated ones. The discrepancy between the results for different $C_2H_2F_4$ cross sections sets is expected since the effective ionization rate is the dominant factor in both timing and efficiency [8]. Somewhat higher efficiency in the $1/n^2$ case is a consequence of larger mean cluster size than in the case of HEED cluster size distribution. It should also be mentioned that the

2014 JINST 9 P09012

tests with different energy distributions for the initial electrons showed no effect on the timing, but the efficiencies were higher by 1-2% in case when mean initial electron energy was set to 10 eV.

4 Summary and conclusions

A microscopic Monte Carlo approach, based on tracking of individual electrons and their collisions with the gas molecules, was developed and used with the aim of obtaining the performance characteristics of a timing RPC. The development of electron avalanches in infinite space was also studied and the results for threshold crossing times showed good agreement with an analytical model. Since the energy distribution of the initial electrons showed no effect on timing, the minor differences can only be attributed to Legler's basic theory of avalanche statistics, assumed in this analytical model.

The realistic RPC simulations with implemented gas gap boundaries and primary ionization models were performed with three different sets of cross sections for electron scattering in $C_2H_2F_4$. The inclusion of boundaries show no significant effect on timing, unlike the effect of different cross section sets which is very prominent. Overall, the results for timing and efficiency show good agreement with experimental values. Because of limited computing resources, a relatively low value of signal threshold was chosen corresponding to about 10^6 electrons in the gas gap. Still, the results can be considered valid as the theory and experiments show that the timing resolution does not depend on the threshold level. The extension of the threshold to realistic levels where space charge is present, without sacrifice in accuracy, is an ongoing work.

Acknowledgments

This work was supported by MPNTRRS Projects OI171037 and III41011.

References

[1] R. Santonico and R. Cardarelli, *Development of resistive plate counters*, *Nucl. Instrum. Meth.* **187** (1981) 377.

[2] R. Santonico, R. Cardarelli, A. Di Biagio and A. Lucci, *Progress in Resistive Plate Counters*, *Nucl. Instrum. Meth.* **A 263** (1988) 20.

[3] ATLAS collaboration, *The ATLAS experiment at the CERN LHC*, 2008 *JINST* **3** S08003.

[4] ALICE collaboration, *The ALICE experiment at the CERN LHC*, 2008 *JINST* **3** S08002.

[5] CMS collaboration, *The CMS experiment at the CERN LHC*, 2008 *JINST* **3** S08004.

[6] P. Fonte, *Applications and new developments in resistive plate chambers*, *IEEE Trans. Nucl. Sci.* **49** (2002) 881.

[7] G. Georgiev et al., *Multigap RPC for PET: development and optimisation of the detector design*, 2013 *JINST* **8** P01011.

[8] P. Fonte, *Survey of physical modelling in Resistive Plate Chambers*, 2013 *JINST* **8** P11001.

[9] W. Riegler and C. Lippmann, *The physics of resistive plate chambers*, *Nucl. Instrum. Meth.* **A 518** (2004) 86.

2014 JINST 9 P09012

[10] S. Mohammed, R. Hasan, N. Majumdar, S. Mukhopadhyay and B. Satyanarayana, *Simulation studies on the Effect of SF_6 in the RPC gas mixture*, PoS(RPC2012)034.

[11] L. Khosravi Khorashad, A. Moshaii and S. Hosseini, *Fast and total charges in a resistive plate chamber: a numerical approach*, *Europhys. Lett.* **96** (2011) 45002.

[12] A. Moshaii, L. Khosravi Khorashad, M. Eskandari and S. Hosseini, *RPC simulation in avalanche and streamer modes using transport equations for electrons andions*, *Nucl. Instrum. Meth.* **A 661** (2012) S168.

[13] W. Riegler, *Time response functions and avalanche fluctuations in resistive plate chambers*, *Nucl. Instrum. Meth.* **A 602** (2009) 377.

[14] A. Mangiarotti, P. Fonte and A. Gobbi, *Exactly solvable model for the time response function of RPCs*, *Nucl. Instrum. Meth.* **A 533** (2004) 16.

[15] S.F. Biagi, *Monte Carlo simulation of electron drift and diffusion in counting gases under the influence of electric and magnetic fields*, *Nucl. Instrum. Meth.* **A 421** (1999) 234.

[16] S. Biagi, *MAGBOLTZ — Program to compute electron transport parameters in gases*, version 2, CERN.

[17] D. Gonzalez-Diaz and A. Sharma, *Current challenges and perspectives in resistive gaseous detectors: a manifesto from RPC 2012*, PoS(RPC2012)084.

[18] H. Schindler, S.F. Biagi and R. Veenhof, *Calculation of gas gain fluctuations in uniform fields*, *Nucl. Instrum. Meth.* **A 624** (2010) 78.

[19] I.B. Smirnov, *Modeling of ionization produced by fast charged particles in gases*, *Nucl. Instrum. Meth.* **A 554** (2005) 474.

[20] I.B. Smirnov, *HEED — Program to compute energy loss of fast particles in gases*, Version 1.01, CERN.

[21] W. Riegler, C. Lippmann and R. Veenhof, *Detector physics and simulation of resistive plate chambers*, *Nucl. Instrum. Meth.* **A 500** (2003) 144.

[22] S. Dujko, Z.M. Raspopović and Z.Lj. Petrović, *Monte Carlo studies of electron transport in crossed electric and magnetic fields in CF_4*, *J. Phys.* **D 38** (2005) 2952.

[23] S. Dujko, R.D. White, K.F. Ness, Z.Lj. Petrović and R.E. Robson, *Non-conservative electron transport in CF_4 in electric and magnetic fields crossed at arbitrary angles*, *J. Phys.* **D 39** (2006) 4788.

[24] S. Dujko, R.D. White and Z.Lj. Petrović, *Monte Carlo studies of non-conservative electron transport in the steady-state Townsend experiment*, *J. Phys.* **D 41** (2008) 245205.

[25] O. Šašić, S. Dupljanin, J. de Urquijo and Z.Lj. Petrović, *Scattering cross sections for electrons in $C_2H_2F_4$ and its mixtures with Ar from measured transport coefficients*, *J. Phys.* **D 46** (2013) 325201.

[26] J. de Urquijo, A.M. Juárez, E. Basurto and J.L. Hernández-Ávila, *Electron swarm coefficients in 1,1,1,2 tetrafluoroethane (R134a) and its mixtures with Ar*, *Eur. Phys. J.* **D 51** (2009) 241.

[27] I.B. Lima et al., *Experimental investigations on the first Townsend coefficient in pure isobutane*, *Nucl. Instrum. Meth.* **A 670** (2012) 55.

[28] D. Bošnjaković, S. Dujko and Z.Lj. Petrović, *Electron transport coefficients in gases for Resistive Plate Chambers*, in proceedings of the 26th *Summer School and International Symposium on the Physics of Ionized Gases*, August 27, Zrenjanin, Serbia (2012).

2014 JINST 9 P09012

[29] H. Itoh, *Electron transport coefficients in SF_6*, *J. Phys.* **D 26** (1993) 1975.

[30] S. Ramo, *Currents induced by electron motion*, *Proc. I.R.E.* **27** (1939) 584.

[31] R.E. Robson, *Transport phenomena in the presence of reactions: definition and measurement of transport coefficients*, *Aust. J. Phys.* **44** (1991) 685.

[32] S. Dujko, R.D. White, Z.M. Raspopović and Z.Lj. Petrović, *Spatially resolved transport data for electrons in gases: definition, interpretation and calculation*, *Nucl. Instrum. Meth.* **B 279** (2012) 84.

[33] S. Dujko, Z.M. Raspopović, Z.Lj. Petrović and T. Makabe, *Negative mobilities of electrons in radio frequency fields*, *IEEE Trans. Plasma Sci. PS* **31** (2003) 711.

[34] W. Legler, *Die Statistik der Elektronenlawinen in elektronegativen Gasen bei hohen Feldstärken und bei grosser Gasverstärkung*, *Z. Naturforsch.* **16a** (1961) 253.

[35] H. Raether, *Electron avalanches and breakdown in gases*, Butterworths, London U.K. (1964).

[36] W. Legler, *The influence of the relaxation of the electron energy distribution on the statistics of electron avalanches*, *Br. J. Appl. Phys.* **18** (1967) 1275.

[37] L. Lopes, P. Fonte and A. Mangiarotti, *Systematic study of gas mixtures for timing RPCs*, *Nucl. Instrum. Meth.* **A 661** (2012) S194.

2014 JINST 9 P09012